AGU PUBLICATIONS

JGR

Journal of Geophysical Research: Atmospheres

RESEARCH ARTICLE

10.1002/2014JD022962

Key Points:
- A latitudinal shift in carbon uptake of 1 PgC/yr using GOSAT
- The shift carbon uptake is not supported by background surface measurements
- Spread in results explained by satellite retrievals and inverse models

Supporting Information:
- Figures S1-S4
- Table S1
- Data S1
- Data S2

Correspondence to:
S. Houweling,
s.houweling@sron.nl

Citation:
Houweling, S., et al. (2015), An intercomparison of inverse models for estimating sources and sinks of CO_2 using GOSAT measurements, *J. Geophys. Res. Atmos.*, *120*, 5253–5266, doi:10.1002/2014JD022962.

Received 15 DEC 2014
Accepted 13 APR 2015
Accepted article online 7 MAY 2015
Published online 29 MAY 2015

An intercomparison of inverse models for estimating sources and sinks of CO_2 using GOSAT measurements

S. Houweling[1,2], D. Baker[3], S. Basu[4], H. Boesch[5], A. Butz[6], F. Chevallier[7], F. Deng[8], E. J. Dlugokencky[4], L. Feng[9], A. Ganshin[10], O. Hasekamp[1], D. Jones[8], S. Maksyutov[11], J. Marshall[12], T. Oda[4,13,14], C. W. O'Dell[15], S. Oshchepkov[11], P. I. Palmer[9], P. Peylin[7], Z. Poussi[16], F. Reum[12], H. Takagi[11], Y. Yoshida[11], and R. Zhuravlev[10]

[1]SRON Netherlands Institute for Space Research, Utrecht, Netherlands, [2]Institute for Marine and Atmospheric Research Utrecht, Utrecht, Netherlands, [3]CIRA, Colorado State University, Boulder, Colorado, USA, [4]NOAA ESRL, Boulder, Colorado, USA, [5]Department of Physics and Astronomy, University of Leicester, Leicester, UK, [6]Karlsruhe Institute of Technology, Karlsruhe, Germany, [7]Le Laboratoire des Sciences du Climat et l'Environnement, Gif-Sur-Yvette, France, [8]Department of Physics, University of Toronto, Toronto,Ontario, Canada, [9]School of GeoSciences, University of Edinburgh, Edinburgh, UK, [10]Central Aerological Observatory, Dolgoprudny, Russia, [11]National Institute for Environmental Studies, Tsukuba, Japan, [12]Max Planck Institute for Biogeochemistry, Jena, Germany, [13]NASA Goddard Space Flight Center, Greenbelt, Maryland, USA, [14]Goddard Earth Sciences Technology and Research (GESTAR), Columbia, USA, [15]Department of Atmospheric Science, Colorado State University, Fort Collins, Colorado, USA, [16]Climmod, Orsay, France

Abstract This study presents the outcome of an inverse modeling intercomparison experiment on the use of total column CO_2 retrievals from Greenhouse Gas Observing Satellite (GOSAT) for quantifying global sources and sinks of CO_2. Eight research groups submitted inverse modeling results for the first year of GOSAT measurements. Inversions were carried out using only GOSAT data, a combination of GOSAT and surface measurements, and using only surface measurements. As expected, the most robust flux estimates are obtained at large scales (e.g., within 20% of the annual flux at the global scale), and they quickly diverge toward the scale of the subcontinental TRANSCOM regions and beyond (to >100% of the annual flux). We focus our analysis on a shift in the CO_2 uptake over land from the Tropics toward the Northern Hemisphere Extra tropics of ~1 PgC/yr when GOSAT data are used in the inversions. This shift is largely driven by TRANSCOM regions Europe and Northern Africa, showing, respectively, an increased uptake and release of 0.7 and 0.9 PgC/yr. Inversions using GOSAT data show a reduced gradient between midlatitudes of the Northern Hemisphere and the Tropics, consistent with the latitudinal shift in carbon uptake. However, the reduced gradients degrade the agreement with background aircraft and surface measurements. To narrow the range of inversion-derived flux, estimates will require further efforts to understand the differences not only between the retrieval schemes but also between inverse models, as their contributions to the overall uncertainty are estimated to be of similar magnitude.

1. Introduction

An important goal of carbon cycle research is to quantify the exchange of carbon between land, ocean, and atmosphere on large scales [*Ciais et al.*, 2010; *Peylin et al.*, 2013]. This can be achieved by budgeting the inputs and outputs of carbon to the atmosphere. The methods, commonly referred to as atmospheric inverse modeling, make use of atmospheric measurements of CO_2 to infer the exchange fluxes [*Enting and Newsam*, 1990; *Enting*, 2002; *Peylin et al.*, 2013]. To improve the availability of measurements, remote sensing techniques have been developed for retrieving column-averaged CO_2 mole fractions (XCO_2) from satellites' observed spectral radiances [*Crisp et al.*, 2004; *Yokota et al.*, 2009; *Boesch et al.*, 2011; *Butz et al.*, 2011]. This approach is particularly promising in remote regions, for example, in the Tropics and at high latitudes that are difficult to measure from the ground. The challenge, however, is to measure CO_2 from space at sufficient precision (~1 ppm) and accuracy (<0.5 ppm) [*Ingmann*, 2009; *Buchwitz et al.*, 2011] (with accuracy defined as the systematic component of measurement uncertainty). It has been shown that inverse-modeling-derived CO_2 fluxes are particularly sensitive to systematic errors, with significant impacts even at the sub-ppm level [*Houweling et al.*, 2010; *Basu et al.*, 2013]. This poses a challenge not only to the design of instruments and the retrieval of data but also to the accuracy of transport models.

TANSO-FTS on board the Japanese Greenhouse Gas Observing Satellite (GOSAT) is the first instrument that has been designed to reach sufficient accuracy for estimating surface fluxes [*Yokota et al.*, 2009]. Advances in instrument calibration and retrieval methods led to rapid improvements in data quality over the years [*Oshchepkov et al.*, 2013; *Yoshida et al.*, 2013]. To assess the quality of the GOSAT-retrieved XCO_2 data, comparisons have been made with in situ measurements from the Total Column Carbon Observing Network (TCCON) of on-ground Fourier Transform Spectrometer (FTS) instruments [*Wunch et al.*, 2011]. The results point to precision and accuracies in the range of 1–2 ppm [*Reuter et al.*, 2013; *Oshchepkov et al.*, 2013].

Meanwhile, GOSAT retrievals have been used for estimation of CO_2 sources and sinks in several studies [*Maksyutov et al.*, 2013; *Basu et al.*, 2013; *Saeki et al.*, 2013; *Chevallier et al.*, 2014; *Takagi et al.*, 2014; *Reuter et al.*, 2014; *Deng et al.*, 2014]. As discussed in these papers, sizable differences are found between inversions using surface and satellite data, sometimes exceeding 1 PgC/yr on the subcontinental scale. Concerns are raised that such differences may not be realistic [*Basu et al.*, 2013; *Chevallier et al.*, 2014], motivated in part by strong sensitivities to bias corrections to the satellite data, although independent verification remains difficult in most cases. A few studies [*Basu et al.*, 2013; *Saeki et al.*, 2013; *Chevallier et al.*, 2014] mention meridional shifts in the terrestrial carbon sink when using GOSAT data, but the attribution to specific regions varies. *Chevallier et al.* [2014] report large and opposing biospheric flux adjustments using GOSAT for Europe (>0.5 PgC/yr increased uptake) and Northern Africa (>0.5 PgC/yr increased release) that are broadly consistent with the results of *Basu et al.* [2013]. *Saeki et al.* [2013] also report increased CO_2 release from Northern Africa but attribute the increased uptake in the Northern Hemisphere to Boreal Asia. *Reuter et al.* [2014] concentrate their analysis on an increased uptake over Europe using GOSAT and conclude that the understanding of the European carbon sink has to be revisited. Generally, the inversion-derived fluxes are difficult to compare because of the different time frames of the inversions, differences in the definition of regions, and the measurements used for evaluating their performance.

The primary aim of our model intercomparison is to improve the comparability of the results of GOSAT inversions, to assess the robustness of the derived fluxes, and to investigate any common signals that may point to new evidence brought in by the satellite. For this purpose, the results of GOSAT inversions are compared with the use of only surface measurements, or a combination of satellite and surface measurements. Our experimental setup does not pose any restrictions on the retrieval data set, transport model, or inversion method to be used. As a result, the range of inversion results reflects the overall uncertainty as much as possible, which is an essential requirement for investigating robustness. The experimental protocol that is used by the participants only takes care of obtaining single model contributions that are internally consistent and allow a one-to-one comparison to other models. Because the model submissions differ in several aspects, this experiment is not suitable for tracing back the causes of specific model-to-model differences or to determine the relative importance of specific steps in the data processing chain. However, an attempt will be made to determine the contribution of differences between satellite retrievals and inverse modeling methods to the overall range of results by comparing our results to *Takagi et al.* [2014] who specifically address the impact of retrieval uncertainties. The performance of our inversions is tested using independent measurements from aircraft campaigns and total column measurements from the TCCON network. The results are used as a benchmark to weigh the contributions of individual models in multimodel averages.

This paper is organized as follows: Section 2 describes the experimental protocol, the participating groups, and their inversions. Section 3 presents results of the performance evaluation and weighted averages of inversion-estimated surface fluxes. The inversion results are analyzed further focusing on seasonal cycle amplitudes and the latitudinal gradient (section 4), leading to the main outcomes of this study, which are summarized in section 5.

2. Methods

Inverse modeling calculations have been performed for the period from 1 June 2009 to 1 June 2010. An overview of the groups participating in the experiment, and the models and methods that were used, is given in Table 1. As mentioned earlier, no restrictions were imposed on the use of specific measurements, prior fluxes, or optimization methods. Results were requested for inversions using only GOSAT data, only surface data, and for a combination of surface and GOSAT data (referred to as GOSAT-only, Flask, and GOSAT+Flask). However, as shown in Table 1 not all groups submitted results of GOSAT inversions with and without surface measurements. Inversion-estimated surface fluxes were requested on a common global 1° × 1° grid and

Table 1. General Overview of the Submissions to the Inverse Modeling Intercomparison

Participant	Transport Model	Driving Meteo	Model Resolution	Inversion Method	Measurements	Submissions[a]
CAO	GELCA v1.0	JMA-JCDAS	2.5° × 2.5° × 32 lev	Kalman smoother	PPDF-S, NOAA (60 sites)	GSC
CSU-NOAA	PCTM	GEOS5 5.2.0	0.7° × 0.5° × 40 lev	Variational	ACOSv2.10, NOAA (68 sites)	GSC
LSCE	LMDZ4	ECMWF	3.75° × 1.9° × 39 lev	Variational	ACOSb3.3, NOAA/WC/CE-IP	GS
MPI-BGC	TM3	NCEP	5° × 3.8° × 19 lev	Variational	ACOSv2.10, continuous, flask, and aircraft (52 sites)	GSC
NIES	NIES08.1	JMA-JCDAS	2.5° × 2.5° × 32 lev	Kalman Smoother	NIESL2v02 Globalview (220 sites)	SC
SRON	TM5-4DVAR	EC ERA-Interim	6° × 4° × 60 lev	Variational	RemoteC v2.0, NOAA (60 sites)	GSC
UoE	GEOS-Chem v8.21	GEOS 5.1	5° × 4° × 47 lev	EnKF	UoLv4, Globalview (76 sites)	GSC
UoT	GEOS-Chem	GEOS 5	5° × 4° × 47 lev	Variational	ACOSv2.10, NOAA+EC (72+6 sites)	GSC

[a]G, GOSAT-only; S, Surface-only; C, Combined use of GOSAT and surface measurements.

monthly time resolution, separating the contributions from fossil fuel use, land biosphere, and oceans. The land biosphere fluxes account for land use change, including emissions from biomass burning and wild fires. To evaluate the inversion-optimized fits to the data, data vectors were collected including times, coordinates, and assumed uncertainties of the inverted data as well as the inversion-derived prior and posterior residuals.

As can be seen in Table 1, we have seven different atmospheric transport models, with two groups using GEOS-Chem [*Bey et al.*, 2001]. Notice, however, that besides transport, the GEOS-Chem inversions are quite different, with UoT using the variational approach [*Henze et al.*, 2007] and UoE an ensemble Kalman filter [*Feng et al.*, 2009] applied to 100 land and 44 ocean regions. The Gelca model [*Ganshin et al.*, 2012] uses the Eulerian global model NIES8.1 [*Belikov et al.*, 2011], in combination with the Flexpart 8.0 Lagrangian particle dispersion model [*Stohl et al.*, 2005]. The other models are described in further detail in *Kawa et al.* [2004] (PCTM), *Hourdin et al.* [2006] (LMDz), *Heimann and Körner* [2003] (TM3), and *Krol et al.* [2005] (TM5). Further details about the setups of the inversions, including references, can be found in the supporting information. The use of GOSAT XCO_2 retrievals from ACOS [*O'Dell et al.*, 2012] is most common (5 models), but our ensemble also represents retrievals from RemoteC [*Butz et al.*, 2011], University of Leicester [*Boesch et al.*, 2011], and PPDF-S [*Oshchepkov et al.*, 2012]. For surface measurements the inversions make use of either measurement-derived GLOBALVIEW-CO_2 data set [*GLOBALVIEW-CO2*, 2009] or in situ and flask measurements made available by NOAA-ESRL [*Dlugokencky et al.*, 2013] and the World Data Centre for Greenhouse Gases (WDCGG). Besides NOAA-ESRL, measurements from the following surface networks were used: CSIRO, EC, JMA, SIO, and NIWA (see http://ds.data.jma.go.jp/gmd/wdcggforfurtherinformation).

To evaluate the performance of the inversions, the optimized models were sampled corresponding to the times and coordinates of a selection of aircraft and total column measurements (see Table 2). In section 3, the skill of the model to reproduce these data is used to weigh the contribution of each model in the presented flux averages. As will be explained in further detail in the next section, this weighing is done in several ways to assess to the robustness of averages of posterior fluxes derived from the ensemble of inversions.

3. Results

3.1. Inversion Performance

The performance of the inversions has been tested by analyzing the inversion-optimized concentrations. Figure 1 shows frequency distributions of GOSAT fit residuals for the GOSAT-only and GOSAT+Flask inversions.

Table 2. Measurement Data Sets That Have Been Used for Evaluating Inverse Model Performance

Type	Campaign/Program	Coverage	Reference
Surface measurements	NOAA-ESRL flask network	Global: 108 sites[a]	*Dlugokencky et al.* [2013]
Aircraft measurements	CONTRAIL	Tokyo to Sydney, S.E. Asia, EU, and USA	*Machida et al.* [2008]
Aircraft measurements	NOAA-ESRL flights	Conterminous USA[b]	*Bakwin et al.* [1994]
Aircraft measurements	HIPPO	Pacific	*Wofsy et al.* [2012]
On ground FTS	TCCON	Global: 13 sites	Data release GGG2012 *Wunch et al.* [2011]

[a]Includes also Poker Flat (Alaska), Rarotonga (Pacific Ocean), and Santarem (Brazil).
[b]The sites include ship board measurements in 5° intervals across the Pacific Ocean.

Note that not all modeling groups submitted results for both inversions, which explains why some colors show up only in one of the two panels. The results of the models for which both inversions are available do not show significant differences in shape or width of the frequency distributions between inversions with and without the use of surface measurements. In case surface and satellite data impose conflicting constraints, this could cause the distribution of fit residuals to widen up for the GOSAT+Flask inversion, which is not evident from Figure 1. Some differences between the frequency distributions can be explained by differences in the treatment of the GOSAT measurements in the inversions. For example, NIES uses monthly averaged GOSAT data over 5° × 5° grid boxes, which explains the relatively narrow frequency distribution. Some models, such as SRON, LSCE, and UoT apply a stricter filtering of the GOSAT data than others, which is not clearly reflected in the width of the distribution. Normalizing the residuals by the corresponding data uncertainties leads to some convergence of the curves in Figure 1 indicating that the assumed data uncertainty and the representation of model errors play a role, although this does not change the ordering of the widths. The widths of the frequency distributions closely reflect the data uncertainty that is used, amounting to 1.6 ppm on average. Besides the treatment of the measurements, several other factors influence the size of the fit residuals, such as the size of the state vector and the assumed a priori flux uncertainty.

Further information about the performance of the inversions is obtained by comparing the optimized models to independent measurements (see Figure 2 and Table 2). Independence is guaranteed for the aircraft measurements but a lesser extent for the TCCON and the surface measurements. TCCON data are commonly used to test the GOSAT satellite retrievals, and the surface measurement data set includes sites of the NOAA-ESRL flask network that are used in the Flask and GOSAT+Flask inversions. The impact of this is clearly seen in the corresponding panel of Figure 2, which shows the most pronounced improvement in model skill when surface measurements are included in the inversion. The comparisons to aircraft data do not show significant differences in performance between inversions with and without GOSAT data. The HIPPO and CONTRAIL aircraft measurement programs show rather divers results, with a more pronounced clustering of results per model than per inversion type. For comparison to CONTRAIL, we exclude measurements collected below 5 km to avoid polluted conditions near airports during takeoff and landing. The models show a better agreement

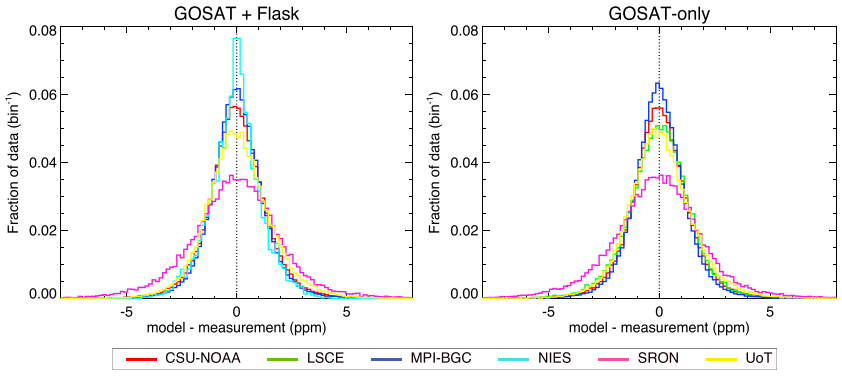

Figure 1. Frequency distributions of fit residuals between GOSAT measurements and inversion-optimized models for inversions (left) using GOSAT in combination with surface measurements and (right) using only GOSAT data.

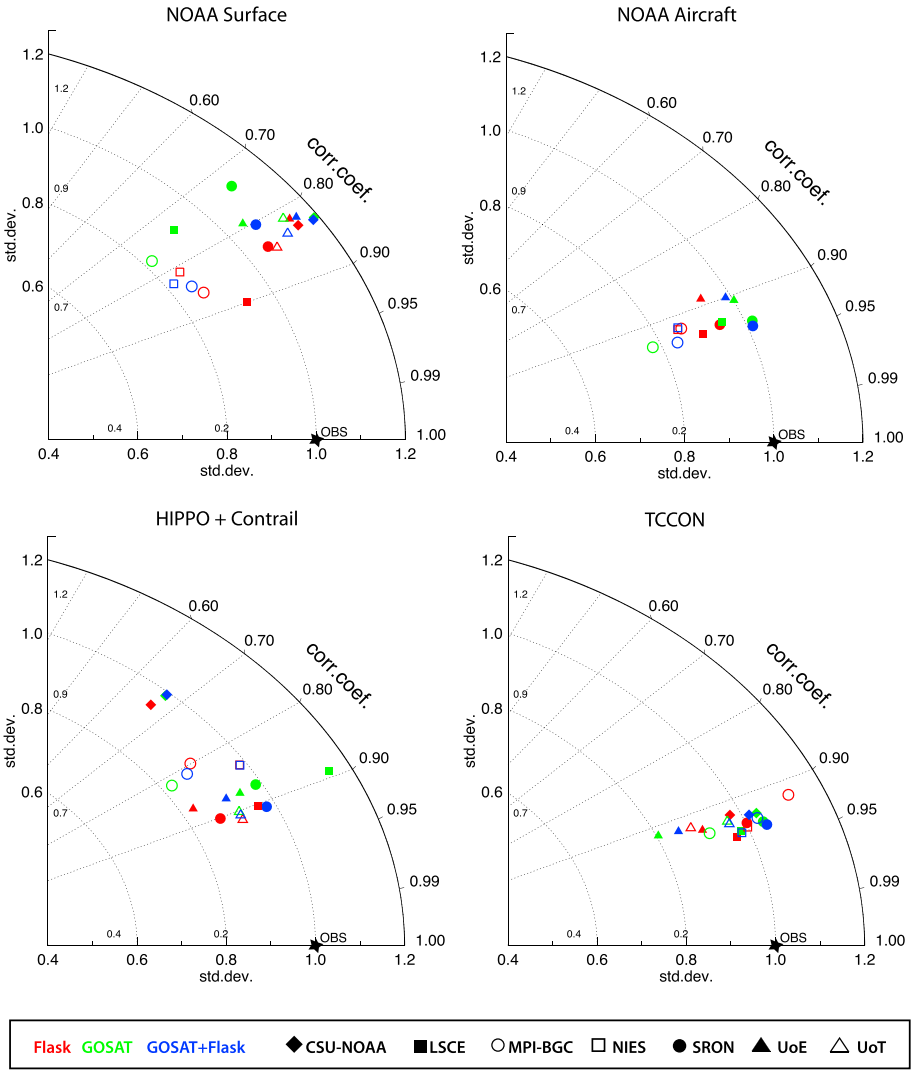

Figure 2. Taylor plots summarizing the performance evaluation of the inversions using independent measurements.

with the NOAA flights than with HIPPO/CONTRAIL, which is explained by the higher altitudes that are reached by the latter and the difficulty to simulate variations in cross tropopause transport. In particular, for the passenger aircraft program CONTRAIL, a large fraction of the data is collected at cruise altitude (i.e., near the tropopause). After filtering out data collected above 10 km, the Taylor plots for HIPPO/CONTRAIL and NOAA look much more similar (not shown). The TCCON total column measurements show the best agreement, but do not discriminate strongly between the approaches. Since GOSAT retrievals are commonly evaluated using TCCON data, a good agreement is expected, in particular, for the RemoTeC retrieval which uses bias corrections based on TCCON data. Note that the performance of the models in the Taylor plots do not correspond to the ordering of the widths of the frequency distribution functions in Figure 1.

As mentioned earlier, the independent data evaluation is used to derive the weights needed to calculate weighted-averaged surface fluxes. Looking at the results in Figure 2, however, there are no obvious systematic differences in the relative performance of the models. Since there is no unique approach to derive the weights, the outcome will depend on the approach that is taken (e.g., on how we weigh the evaluation data themselves). For this reason a few different approaches are taken as explained below, which allow us to test the sensitivity of our results to the weighting method. Table 3 summarizes the weights that were used per model and weighing method.

As can be seen in the table, the weighing method W1 simply applies the same weight to each model. This method makes it difficult to compare the results of the three inversion types, since some groups did not

Table 3. Model Selection and Weighing

Weighing Method	Inversion Type	Weight CAO	CSU-NOAA	LSCE	MPI-BGC	NIES	SRON	UoE	UoT
W1	Flask	1	1	1	1	1	1	1	1
W1	GOSAT	1	1	1	1	0	1	1	1
W1	GOSAT+Flask	1	1	0	1	1	1	1	1
W2	Flask	1	1	0	1	0	1	1	1
W2	GOSAT	1	1	0	1	0	1	1	1
W2	GOSAT+Flask	1	1	0	1	0	1	1	1
W3	Flask	0	1	1	1	1	1	1	0
W3	GOSAT	0	1	1	1	1	1	1	0
W3	GOSAT+Flask	0	1	1	1	1	1	1	0
W4	Flask	0	0.53	0.77	0.56	0.66	0.70	0.65	0.72
W4	GOSAT	0	0.53	0.66	0.63	0	0.69	0.63	0.74
W4	GOSAT+Flask	0	0.53	0	0.62	0.67	0.75	0.65	0.76
W5	Flask	0	0.49	0.80	0.57	0.66	0.74	0.69	0.72
W5	GOSAT	0	0.49	0.65	0.66	0	0.77	0.69	0.74
W5	GOSAT+Flask	0	0.49	0	0.63	0.66	0.81	0.70	0.76

submit results for GOSAT-only and GOSAT+Flask. Weighing method W2 accounts for this problem by including only those models that submitted results for both inversions types. Weighting methods W4 and W5 use the inverse RMS difference between the evaluation data sets and the optimized models as weights. Surface data are excluded from the weighing, because they are not independent of the data that are used in the inversions. Equal weighing of each measurement in the RMS calculation would result in a disproportionally strong weight to the CONTRAIL program. In W4, each aircraft campaign receives equal weight, and the TCCON measurements receive a double weight to balance the aircraft and total column measurements. In W5, programs that deliver more data are assigned a larger weight, but to limit the impact they are weighted by the square root of the number of measurements. Note that the CAO submissions receive no weight in the RMS-based weighing, because they did not submit the evaluation data set. Weighting method W3 excludes models with an identified problem in the evaluation data set (CAO: because no data were available, UoT: because of an incomplete aircraft evaluation data set). Interestingly, the RMS-derived weights W4 and W5 also point out that, on average, combining all independent evaluation data sets (i.e., without the surface data), the inversions using GOSAT data perform slightly better than the inversions using only surface data.

3.2. Posterior Fluxes

Inversion-estimated carbon fluxes are analyzed after integration over the 12 month target period of the experiment (1 June 2009 to 1 June 2010) and integration over a large range of spatial scales. The $1° \times 1°$ scale of the submitted fluxes is not very useful as it shows differences in the region definition and spatial resolution of the underlying models. The comparisons become more interesting after spatial aggregation to the subcontinental regions of the transport model intercomparison project TRANSCOM (see http://transcom.project.asu.edu). These regions were introduced by *Gurney et al.* [2002] and are commonly used for analyzing regional to subcontinental-scale carbon fluxes. For convenience the map of regions is included (see Figure 3). Comparisons of inversion-derived fluxes for each TRANSCOM region can be found in the supporting information.

As expected, the best agreement between the inverse models is found at the largest scales, which are best resolved by the measurements. This is true, in particular, for the global and annual integral, which should reflect the observed annual increase of the background CO_2 mole fraction. The results in Figure 4 confirm that this is the case. The different weighting approaches of Table 3 are shown in different colors. Averaged over all weighting methods, global fluxes decrease by close to 2 PgC/yr compared to the a priori fluxes. This is explained by the use of ecosystem models that are close to carbon neutral on an annual basis, as can be seen in the "Global land" panel of Figure 4.

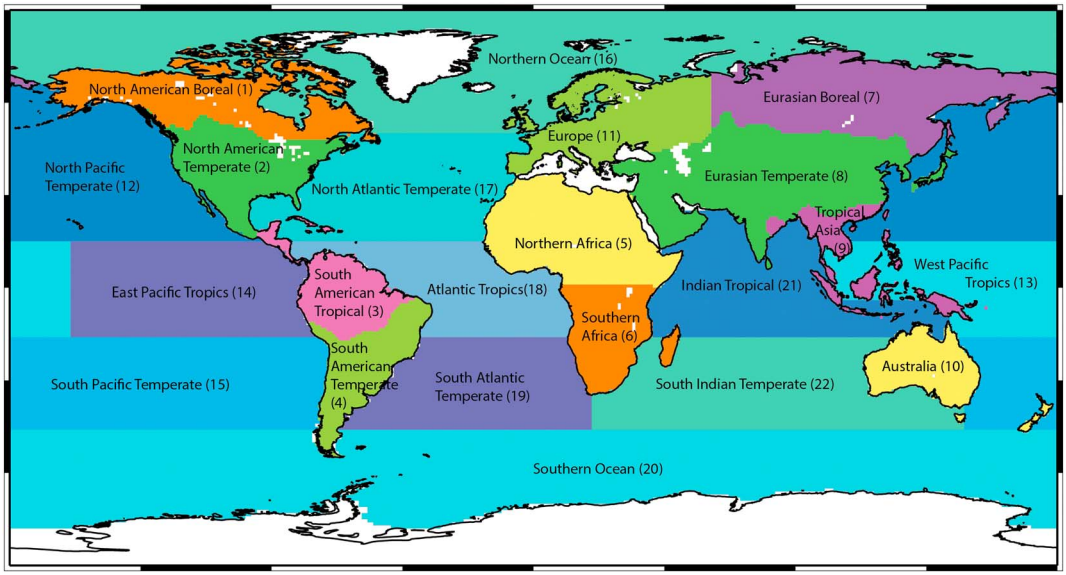

Figure 3. TRANSCOM region map [*Gurney et al.*, 2002] used for integration of subcontinental surface fluxes.

The global uncertainty, as measured by the weighted standard deviation of the models, reduces from 1.7 to 0.5 PgC/yr for the Surface-only inversions. When GOSAT data are added, this uncertainty increases to 0.9 PgC/yr. An uncertainty increase, despite an improvement in the availability of data, points to differences between the statistics of the actual constraints on the inversions (a priori fluxes and measurements), from the assumed uncertainties (as specified in the data and flux error covariance matrices). Toward smaller scales the ratio of flux and uncertainty quickly reduces, for example, from 8.6 on the global scale to 2.2 for the net carbon uptake of the global terrestrial biosphere. On the scale of individual TRANSCOM regions, uncertainties may exceed the fluxes leading to flux/uncertainty ratios smaller than 1, for example, for Eurasian Temperate (0.6), and South American Tropical (0.5). On that scale, ratios vary typically between 0.5 and 2, depending also on the size of the mean flux.

We have compared the standard deviations of the inversion estimates (i.e., the size of the error bars for the GOSAT+Flask inversions in Figure 4) with the corresponding variations in the inversion results of *Takagi et al.* [2014]. The latter represent the impact of using different GOSAT retrievals, when keeping everything else (model, prior fluxes, etc.) the same. The average uncertainty across all the TRANSCOM regions with significant uncertainty reduction due to the use of GOSAT and Surface data is 0.41 TgC/yr in our study, compared to 0.25 TgC/yr in *Takagi et al.* [2014]. The selected regions are those of Figure 3c in *Takagi et al.* [2014], for which the uncertainty reduction exceeds 10%. These are all TRANSCOM land regions except North America Boreal and Temperate, Australia, and Tropical Asia. With an estimate of the total uncertainty and the contribution of the GOSAT retrieval scheme, we can make a rough estimate of the error contribution of all other components of the inversion. If we assume that the retrieval and inversion components are independent, so that they can be combined as squared sums, the contribution of the inversion is about 0.3 TgC/yr, which is comparable or even larger than that of the retrieval.

Comparing inversions with and without the use of GOSAT data, the most salient feature is a shift in the biospheric uptake from the Tropics to temperate and Boreal latitudes of the Northern Hemisphere. To measure this difference, we integrate the TRANSCOM regions "South American Tropical," "Northern Africa," and "Tropical Asia" into a region called "Tropical Land," and the temperate and Boreal regions of North America and Asia together with TRANSCOM region "Europe" into "NH. Extratropical Land." As can be seen in Figure 4 the shift in C uptake between these regions amounts to 0.98 PgC/yr. Judging from the associated uncertainties, this shift may not seem significant. However, as we will show later, the error bars in Figure 4 are highly correlated, concealing a signal that is in fact rather systematic across the models. The TRANSCOM regions that contribute most to the increased uptake in the Extratropical Northern hemisphere are Europe (0.7 PgC/yr), North American Temperate (0.35 Tg/yr), and North America Boreal (0.1 Tg/yr). The increased CO_2 release in the Tropics is dominated by Northern Africa (0.9 Pg/yr), followed by Tropical South America (0.11 Pg/yr), and

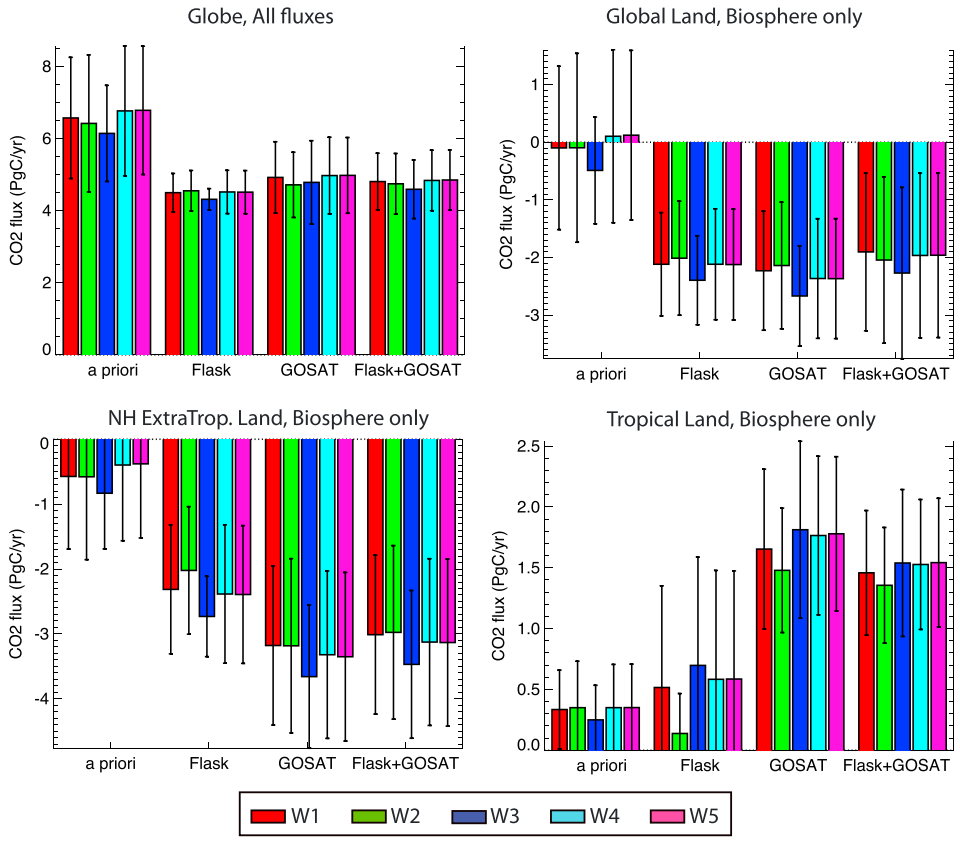

Figure 4. Comparison of inversion-estimated fluxes, with and without GOSAT data, integrated annually (June 2009 to June 2010) and over large-scale regions. The bars represent weighted averages, using the weights of Table 3. The error bars represent the weighted standard deviation of the spatiotemporal integrated posterior fluxes.

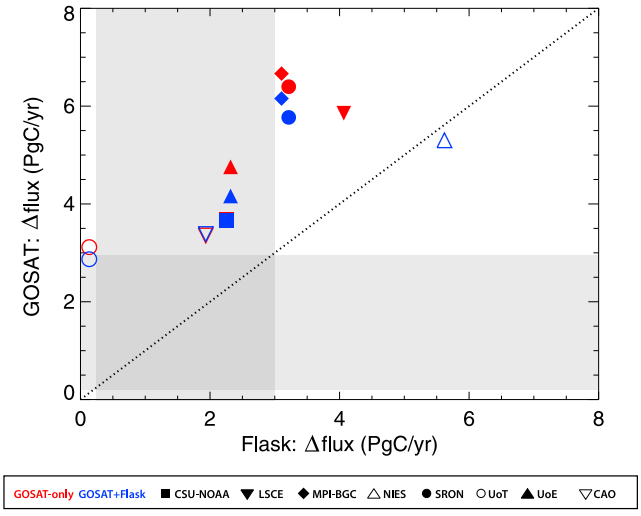

Figure 5. Inversion-derived latitudinal shifts in fluxes (Δflux) comparing GOSAT and Surface inversions. Δflux is defined as the difference in annual biospheric carbon uptake of Tropics minus NH Extra Tropics. The gray zone represents the range in Δflux that is supported by *Stephens et al.* [2007]. In the dark gray zone this is true for corresponding Flask and GOSAT inversions.

Tropical Asia (0.09 PgC/yr). Some of these regional differences are not significant given the range of model estimates. However, the dipole between Northern Africa and Europe is so large that it calls for an explanation.

To demonstrate that the shift in the direction of more tropical carbon release and more temperate and Boreal carbon uptake is indeed systematic, the results are plotted per model and inversion in Figure 5. As can be seen, all models, except NIES, shift the uptake toward higher latitudes. For most models the shift is larger when GOSAT data are taken into account, except for NIES which shows large shifts already in the Surface-only inversion. Based on aircraft profile measurements, *Stephens et al.* [2007] constrained the ratio between tropical and extratropical carbon uptake. The range of fluxes supported by this study is indicated

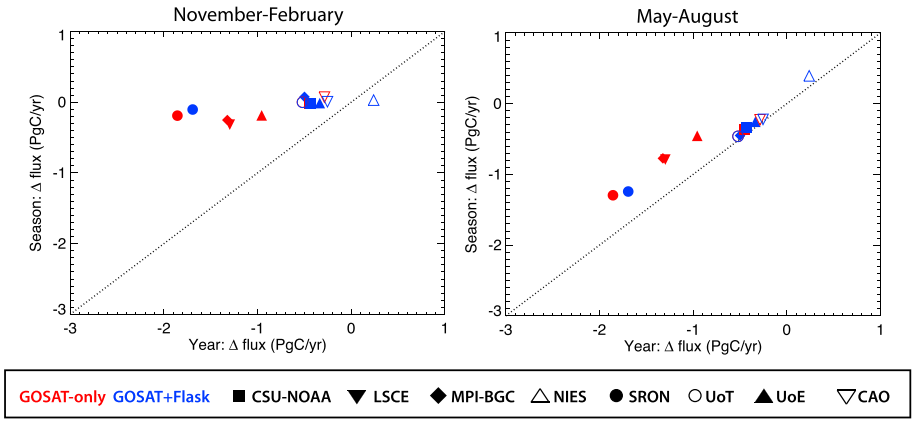

Figure 6. Relationship between annual and seasonal CO_2 uptake for TRANSCOM region Europe, for the seasons (left) November to February and (right) May to August. Δflux is defined as the difference in biospheric carbon uptake between GOSAT and Surface-only inversions (GOSAT minus Surface).

by the gray bands in Figure 5. Only three of our Surface-only inversions satisfy this constraint, with three others just outside the gray band. Adding GOSAT data, all the inversion move further away from the *Stephens et al.* [2007] supported range except for the UoT and NIES GOSAT+Flask inversions.

To further investigate the cause of the increased carbon uptake in the Northern Hemisphere as derived from GOSAT we focus our attention on the European-African dipole, as it seems to be a key driver of this phenomenon. We verified that the dipole is systematic across models, by plotting the corresponding fluxes in the format of Figure 5. A similar relationship is found (not shown), with a mean shift in the annual flux of 0.8 ± 0.7 PgC/yr. Figure 6 separates the sink over Europe into its seasonal components. Plotting the difference with and without the use of GOSAT data results in tight relationships, demonstrating that the increased sink is explained primarily by increased carbon update during summer. Note that "summer" is defined rather loosely as the period from May to August. This choice is motivated by the wish to combine months when the GOSAT data coverage at European latitudes is relatively favorable. Likewise, the "winter" months, from November to February, are those for which the opposite is true. To facilitate the interpretation of this figure a one-to-one line is plotted. The distance from this line is a measure of the fraction of the annual sink that is explained by the respective seasons. As can be seen in Figure 6, results for the May to August period stay close to this line, whereas the results for November to February have almost no component in this direction. We varied the selection of months to investigate whether this results is particularly sensitive to a specific month, which turns out not to be the case (not shown). The question remains whether this result has any implications for the GOSAT-induced strengthening of the carbon uptake in the NH Extratropics, which will be discussed further in the next section.

4. Discussion

In this section, we will attempt to answer the question whether the GOSAT-induced shift in carbon uptake from the Tropics to the Northern Hemispheric Extratropics might be real, despite the fact that this shift brings their ratio outside the *Stephens et al.* [2007] supported range. Meanwhile, we have narrowed down the main origin of the shift to the European summer. An increased carbon uptake over Europe using GOSAT data is consistent with recent studies by *Chevallier et al.* [2014] and *Reuter et al.* [2014]. The latter study isolated the influence of GOSAT data over Europe, which implies that the strengthened uptake is driven by regional rather than large-scale observational constraints. Their estimate of the European biospheric sink of 1.03 ± 0.3 PgC/yr for 2010 is rather consistent with what we find for June 2009 to June 2010 (1.03 ± 0.47 PgC/yr and 1.43 ± 0.66 PgC/yr for GOSAT inversions, respectively, with and without the use of surface data). Unlike *Reuter et al.* [2014], who only verify their results using independent data within the European domain, we can investigate the extent to which an increased carbon uptake at midlatitude to high latitude is supported by observational constraints on background concentrations at large scales.

First, we investigate the relation between the vertical gradient of CO_2 at midlatitudes of the Northern Hemisphere and the annual CO_2 exchange over Tropical and NH Extratropical land, similar to the approach

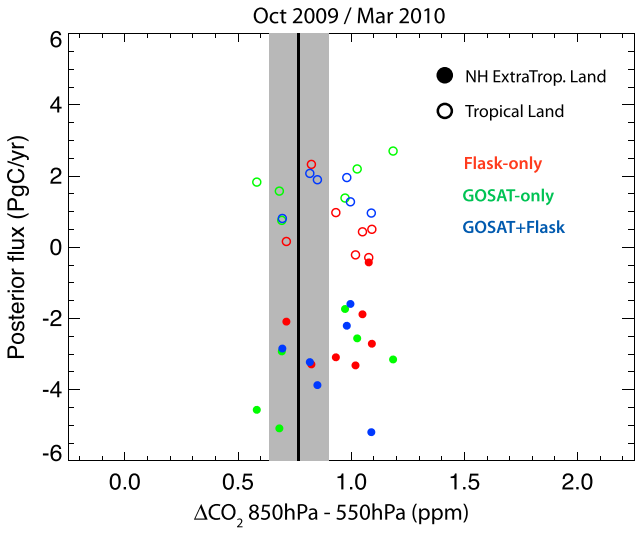

Figure 7. Comparison between simulated and observed vertical gradients of CO_2, and their relationship with inversion-derived carbon fluxes. Each circle represents a flux estimate from an individual inversion. The black vertical line and gray bar represent the mean and range of vertical profiles that are supported by HIPPO aircraft measurements between 30°N and 60°N, collected during HIPPO 2 (October 2009) and HIPPO 3 (March 2010). ΔCO_2 denotes the difference in CO_2 between 900–800hPa and 700-400hPa.

that was used in *Stephens et al.* [2007] (referred to as S07 further on). For our experiment, the availability of useful aircraft measurements is limited to the HIPPO campaigns that took place within the time window of our experiment (HIPPO 2, October 2009; HIPPO 3, March 2010). The results are plotted in Figure 7, which is equivalent to Figure 3b in S07 except that we have a poorer sampling of the annual mean. This is expressed by the gray bar, representing the uncertainty of the measured vertical profile, which is wider than in S07. To improve the statistics we do not evaluate the CO_2 difference at 1 and 4 km altitude like in S07, but between the ranges 900–800 hPa and 700–400 hPa. We do acknowledge that we have only a rather poor seasonal sampling, which prevents a one-to-one comparison with S07. Still, it is a useful reference for other comparisons that follow later in this section.

According to S07, inversions that match the observed latitudinal gradient of CO_2 at the surface show a clear relationship between the CO_2 exchange in the Tropics and northern latitudes that is determined by vertical mixing in the model. Differences in vertical mixing modify the vertical gradient of CO_2, which is tested using aircraft measurements, thus providing a constraint on the ratio between tropical and extratropical carbon fluxes. Models that classify as realistic in S07 show a relatively weak uptake of −1.5 PgC/yr at northern latitudes combined with a weak tropical emission of 0.1 PgC/yr. Our results (see Figure 7) show relationships that are less tight, which can be explained by the fact that the inversions use different measurements, different prior fluxes, etc. In addition, the observed vertical profiles are reproduced with a much larger northern latitude carbon uptake (around 4 PgC/yr) and tropical release (up to 2 PgC/yr). For the GOSAT-only inversions this could imply that they do not satisfy the latitudinal gradient as observed by the ground-based network. However, since the GOSAT+Flask inversions are optimized to satisfy that constraint and result in latitudinally shifted uptakes also, there must be another explanation.

One possibility is a difference in the meridional gradient between the boundary layer and the free troposphere, which are constrained in a different way by the surface and satellite data. Again the vertical profiles measured during the HIPPO campaigns offer an excellent validation opportunity. To investigate this, modeled and measured samples between 900 hPa and 300 hPa were averaged over 30°N–60°N and 30°S–30°N. The difference between these latitudinal bands is plotted in Figure 8. The results point to a reduction in the north-south gradient of CO_2 when GOSAT data are used, although there is no clear relationship with the inversion-derived fluxes for Tropical Land and the NH. Extratropical Land. The reduced north-south gradients of CO_2 drift outside the HIPPO supported range, indicating that inversions using GOSAT data perform less well in this test. It would be interesting to know whether this is caused by the intrahemispheric transport in the models, or by the GOSAT retrievals. Our free format intercomparison experiment is not well suited to isolate the role of model transport, but it would be an interesting target for future intercomparisons.

The results in Figure 8 raise the question how well the GOSAT+Flask inversions reproduce the meridional gradient of CO_2 as observed near the surface. Furthermore, a potentially important degree of freedom in our comparison is longitudinal variation. The large distance between the HIPPO measurements over the Pacific and the centers of action in our inversions, located in Europe and Northern Africa, likely weakens the connection between vertical CO_2 gradients and meridional flux differences. To address these questions, a similar comparison as in Figure 8 has been made using surface measurements from NOAA-ESRL (see Figure 9),

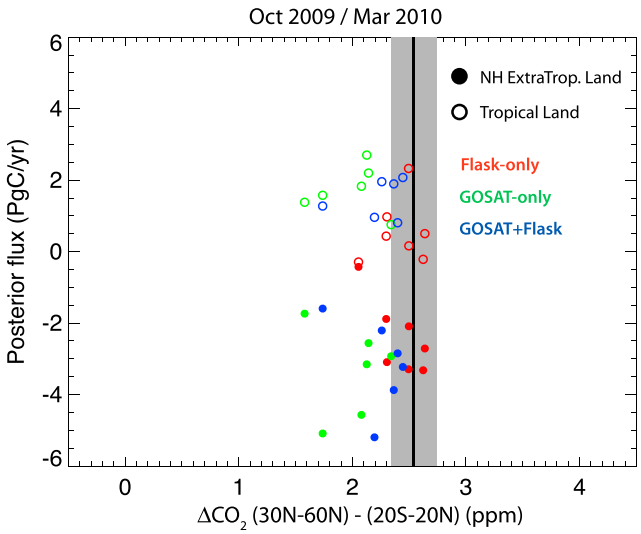

Figure 8. Comparison between simulated and measured meridional gradients of CO_2, and their relationship with inversion-derived carbon fluxes. The black vertical line and gray bar represent the mean and range of meridional gradients that are supported by HIPPO aircraft measurements between 900 hPa and 300 hPa collected during HIPPO 2 (October 2009) and HIPPO 3 (March 2010). ΔCO_2 denotes the difference in CO_2 between 30°N–60°N and 20°S–20°N.

spanning a wide range in longitude. For this purpose, background sites were selected in the Tropics (sites ASC, ASK, GMI, MLO, RPB, SMO, SEY, and MKN) and the Northern Hemisphere Extratropics (sites ALT, BRW, CBA, ICE, SHM, STM, SUM, and ZEP), including sites in the Arctic, Atlantic, and Indian Oceans. The results (Figure 9) show that several inversions using GOSAT data end up outside the range that is supported by the measurements, like in the comparison with HIPPO data.

The uncertainty range requires some further attention, because the difference between the tropical and high-latitude measurements varies with season. This is a signal that is resolved by the data and therefore does not reflect measurement uncertainty, although it limits our ability to quantify the annual mean latitudinal difference. Since the models are sampled just like the surface measurements, the seasonal variability does not influence the uncertainty of the mean difference between model and measurement. It explains why most of the surface-only inversions end up well within the 1σ range of Figure 8. The observational uncertainty in the difference between tropical and high-latitude samples is rather determined by the accuracy of the sampling network, which should be within 0.2 ppm. As can be seen in Figure 8, most of the GOSAT-only and GOSAT+Flask inversions do not satisfy that constraint. Compared with Figure 8, GOSAT inversions show a somewhat clearer relationship between Tropical and Extratropical fluxes and CO_2 gradients, favoring combinations of lower Tropical carbon release and lower Extratropical uptake, although there is still a sizable scatter. Overall, our results indicate that the GOSAT-induced push toward higher Northern Hemispheric carbon uptake does not improve the consistency between the inversion-optimized atmospheric states and in situ measurements.

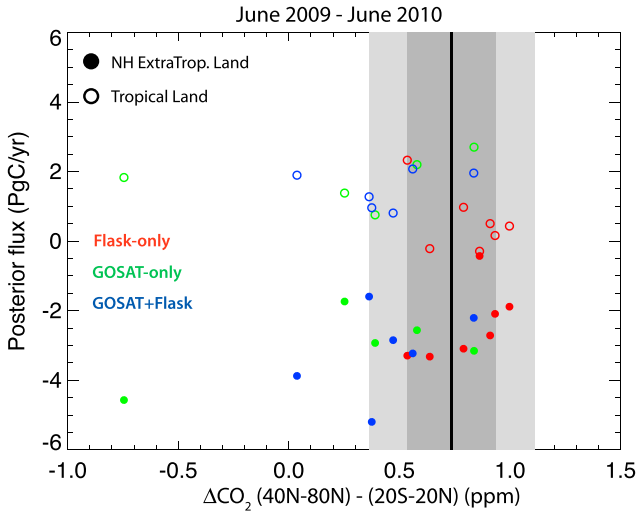

Figure 9. As Figure 8 for surface measurements from background sites from the NOAA-ESRL flask sampling network in the period June 2009 to June 2010. The black vertical line and light gray bar represent the mean and 1σ uncertainty of meridional gradients derived from the surface measurements. The dark gray band represents systematic uncertainties in the data. ΔCO_2 denotes the difference in CO_2 from sites between 40°N–80°N and 20°S–20°N.

A possible explanation for this result is the seasonal variation in coverage of GOSAT, which varies with latitude following solar insolation. As a result, the data impose a stronger constraint on the European biosphere in summer than in winter. This way, an offset in the annual mean XCO_2 between retrieved and model simulated GOSAT data would have a stronger impact during summer than during winter, which may disturb the annual balance

between growth and respiration causing an artificial sink. The potential importance of sampling biases in inverse modeling applications of satellite data was confirmed in a synthetic study by *Liu et al.* [2014].

Even if the increased uptake during summer is real, the annual uptake may still be influenced by a seasonal sampling bias. Because of the tight correlation between photosynthesis and respiration, a stronger production during summer is likely compensated, to some extent, by a stronger respiration during winter. However, if the latter is not, or less well observed, the winter season flux would stay close to the prior. The inversion setups that are used could be made less sensitive to such a sampling bias, by accounting for the relationship between productivity and respiration in the prior flux covariance matrix. This way, the optimal solution would show increased wintertime respiration in response to an increased summer uptake in the absence of measurements during winter.

If our models, which do not account for such correlations, underestimate winter time respiration over Europe, then this may be tested using independent data. We have investigated the modeled and observed seasonal cycles of XCO_2 at the European TCCON sites Bialystok, Garmisch, and Bremen. This choice was motivated by the Taylor plot for TCCON in Figure 2. The narrow range of correlations between models and data reflects a dominant role of the seasonal cycle. Given the importance of seasonality, the wide range in modeled standard deviations could reflect differences in seasonal amplitude. However, upon closer inspection of the inversion-optimized seasonal cycles at the European TCCON sites, we find that short-term variations in XCO_2 play an important role also (not shown). Because of this the comparisons show too much scatter to verify a possible impact of sampling bias on the seasonal amplitude. There is also no clear relationship between the standard deviations in the TCCON panel of Figure 2 and the corresponding annual carbon uptakes over Europe.

5. Conclusions and Recommendations

The inverse modeling technique provides a consistent statistical framework for combining information about surface fluxes and atmospheric mole fractions of CO_2 to derive improved flux estimates. Inverse modeling intercomparisons are important for assessing the importance of sources of uncertainty, such as transport model uncertainties, that are difficult to account for in a single inversion. In addition, the free format of our experiments, allowing among others the use of different GOSAT retrieval products, also accounts for uncertainties of satellite retrievals that are difficult to quantify within a single retrieval scheme or in comparison with TCCON measurements. By evaluating the performance of inversions using independent data, we avoid that our uncertainty ranges reflect that of the less realistic extremes, although the performances of our inversions turned out to be rather comparable. On the scale of TRANSCOM regions, many features that show up in single inversions prove not to be robust, as compared with the uncertainty of the weighted means. The most robust signal is a shift in the annual CO_2 uptake over land of ~1 PgC/yr from the Tropics to the Northern Hemisphere Extratropics.

This result is dominated by contributions from TRANSCOM regions Europe (0.7 PgC/yr increased uptake) and Northern Africa (0.9 PgC/yr increased release). However, it remains difficult to confirm the validity of it using independent data. A possible cause of the increased biospheric uptake over Europe is the seasonally varying measurement coverage of GOSAT measurements at midlatitude to high latitude of the Northern Hemisphere. As expected in this case, the increased annual carbon sink is largely explained by flux corrections during late spring and summer, when the data coverage is best. Compensating increases in respiration during winter may not be represented well enough by the limited available data during this season. The inversion methods that are used in this study are expected to be sensitive to spatiotemporal variations in measurement coverage. Currently, however, the evidence of sampling biases playing an important role is still limited, since the available TCCON data during winter do not show a significant sign of underestimated XCO_2 in GOSAT-optimized models that show a large annual uptake of CO_2 over Europe. Nevertheless, the sensitivity of inverse modeling results to the seasonally varying measurement coverage of satellites should be investigated in further detail.

Comparisons of measured and inversion-optimized meridional gradients in background CO_2 show that inversions using GOSAT data tend to underestimate this gradient, indicating that the shift in carbon uptake toward higher latitudes of at least some of these models is not supported by in situ measurements. The range of results obtained using different models also points to possibility of transport model uncertainties playing an important role. By combining the results of our study with those of *Takagi et al.* [2014], we derive a comparable contribution of models and satellite retrievals to the overall uncertainty. Since the evidence for this is still

rather indirect, comparing results of different studies, it would be useful to quantify this further in a future model intercomparison experiment. For such a study it will be important to use more years of GOSAT data, to shed further light on its tendency to strengthen the inversion-derived carbon uptakes in the Northern Hemisphere Extratropics in general, and over Europe in particular.

Acknowledgments

This study made use of several measurement data sets that were kindly made available to us and are essential for our research, including: HIPPO (http://hippo.ucar.edu), CONTRAIL (http://www.cger.nies.go.jp/contrail/contrail.html), NOAA aircraft profiles (http://www.esrl.noaa.gov/gmd/ccgg/aircraft/), TCCON (http://www.tccon.caltech.edu), and various surface measurement networks (CSIRO, EC, Niwa, JMA, and LSCE) who make their data available through the World Data Centre for Greenhouse Gases (http://ds.data.jma.go.jp/gmd/wdcgg/). We would like to thank the GOSAT project for making the GOSAT-observed spectral radiances freely available. In addition, we thank the organizers of GOSAT RA to stimulate international collaboration by organizing meetings, which initiated this intercomparison initiative. University of Leicester, SRON and KIT received funding from ESA via the GHG-CCI project.

References

Bakwin, P. S., et al. (1994), In climate monitoring and diagnostics laboratory GMD, *Tech. Rep. NO. 22 Summary Report*, edited by J. T. Peterson and R. M. Rosson, pp 18–30, NOAA-ESRL, Boulder, Colo.

Basu, S., et al. (2013), Global CO_2 fluxes estimated from GOSAT retrievals of total column CO_2, *Atmos. Chem. Phys.*, *13*, 8695–8717, doi:10.5194/acp-13-8695-2013.

Belikov, D., S. Maksyutov, T. Miyasaka, T. Saeki, R. Zhuravlev, and B. Kiryushov (2011), Mass-conserving tracer transport modelling on a reduced latitude-longitude grid with NIES-TM, *Geosci. Model Dev.*, *4*, 207–222.

Bey, I., D. J. Jacob, R. M. Yantosca, J. A. Logan, B. D. Field, A. M. Fiore, Q. Li, H. Y. Liu, L. J. Mickley, and M. G. Schulz (2001), Global modeling of tropospheric chemistry with assimilated meteorology: Model description and evaluation, *J. Geophys. Res.*, *106*, 23,073–23,095.

Boesch, H., D. Baker, B. Connor, D. Crisp, and C. Miller (2011), Global characterization of CO_2 column retrievals from shortwave-infrared satellite observations of the Orbiting Carbon Observatory-2 Mission, *Remote Sens.*, *3*, 270–304, doi:10.3390/rs3020270.

Buchwitz, M., F. Chevallier, P. Bergamaschi, I. Aben, H. Bösch, O. Hasekamp, J. Notholt, and M. Reuter (2011), User Requirements Document (URD) for the GHG-CCI project of ESA's climate change initiative, *Tech. Rep.*, 45 pp., ver. 1, ESA. [Available at http://www.esa-ghg-cci.org, last access: 5 June 2014.]

Butz, A., et al. (2011), Toward accurate CO_2 and CH_4 observations from GOSAT, *Geophys. Res. Lett.*, *38*, L14812, doi:10.1029/2011GL047888.

Chevallier, F., P. I. Palmer, L. Feng, H. Boesch, C. W. O'Dell, and P. Bousquet (2014), Toward robust and consistent regional CO_2 flux estimates from in situ and spaceborne measurements of atmospheric CO_2, *Geophys. Res. Lett.*, *41*, 1065–1070, doi:10.1002/2013GL058772.

Ciais, P., A. J. Dolman, R. Dargaville, L. Barrie, A. Bombelli, J. Butler, P. Canadell, and T. Moriyama (2010), *Geo Carbon Strategy*, Geo Secretariat Geneva,/FAO, Rome.

Crisp, D., et al. (2004), The orbiting carbon observatory (OCO) mission, *Adv. Space. Res.*, *34*, 700–709.

Deng, F., et al. (2014), Inferring regional sources and sinks of atmospheric CO_2 from GOSAT XCO_2 data, *Atmos. Chem. Phys.*, *14*, 3703–3727, doi:10.5194/acp-14-3703-2014.

Dlugokencky, E. J., P. M. Lang, K. A. Masarie, A. M. Crotwell, and M. J. Crotwell (2013), Atmospheric carbon dioxide dry air mole fractions from the NOAA ESRL carbon cycle cooperative global air sampling network, 1968–2012, version 2013-08-28, *Tech. Rep.*, NOAA–ESRL, Boulder, Colo. [Available at ftp://aftp.cmdl.noaa.gov/data/trace_gases/co2/flask/surface/.]

Enting, I. (2002), *Inverse Problems in Atmospheric Constituent Transport*, Cambridge Univ. Press, Cambridge, U. K.

Enting, I. G., and G. N. Newsam (1990), Atmospheric constituent inversion problems: Implications for baseline monitoring, *J. Atmos. Chem.*, *11*, 69–87.

Feng, L., P. I. Palmer, H. Bösch, and S. Dance (2009), Estimating surface CO_2 fluxes from space-borne CO_2 dry air mole fraction observations using an ensemble Kalman Filter, *Atmos. Chem. Phys.*, *9*, 2619–2633.

Ganshin, A., et al. (2012), A global coupled Eulerian-Lagrangian model and 1 1 km CO_2 surface flux dataset for high-resolution atmospheric CO_2 transport simulations, *Geosci. Model Dev.*, *5*, 231–243.

GLOBALVIEW-CO2 (2009), *Cooperative Atmospheric Data Integration Project-Carbon Dioxide, CD-ROM*, NOAA-ESRL, Boulder, Colo. [Also available on Internet via anonymous FTP to ftp.cmdl.noaa.gov,Path:ccg/co2/ GLOBALVIEW.]

Gurney, K. R., et al. (2002), Towards robust regional estimates of CO_2 sources and sinks using atmospheric transport models, *Nature*, *415*, 626–630.

Heimann, M., and S. Körner (2003), The global atmospheric tracer model TM3: Model description and user's manual Release 3.8a, *Tech. Rep. No. 5*, Max Planck Institute of Biogeochemistry, Germany.

Henze, D. K., A. Hakami, and J. H. Seinfeld (2007), Development of the adjoint of GEOS-Chem, *Atmos. Chem. Phys.*, *7*, 2413–2433.

Hourdin, F., et al. (2006), The LMDZ4 general circulation model: Climate performance and sensitivity to parametrized physics with emphasis on tropical convection, *Clim. Dyn.*, *27*, 787–813.

Houweling, S., et al. (2010), The importance of transport model uncertainties for the estimation of CO_2 sources and sinks using satellite measurements, *Atmos. Chem. Phys.*, *10*, 9981–9992, doi:10.5194/acp-10-9981-2010.

Ingmann, P. (2009), *A-SCOPE, Advanced Space Carbon and Climate Observation of Planet Earth*, Report for Assessment, SP-1313/1, ESA Communication Production Office, Noordwijk, Netherlands.

Kawa, S. R., D. J. Erickson III, S. Pawson, and Z. Zhu (2004), Global CO_2 transport simulations using meteorological data from the NASA data assimilation system, *J. Geophys. Res.*, *109*, D18312, doi:10.1029/2004JD004554.

Krol, M., S. Houweling, B. Bregman, M. van den Broek, A. Segers, P. van Velthoven, W. Peters, F. Dentener, and P. Bergamaschi (2005), The two-way nested global chemistry-transport zoom model TM5: Algorithm and applications, *Atmos. Chem. Phys.*, *5*, 417–432.

Liu, J., et al. (2014), Carbon monitoring system flux estimation and attribution: Impact of ACOS-GOSAT XCO_2 sampling on the inference of terrestrial biospheric sources and sinks, *Tellus B*, *66*, 22,486, doi:10.3402/tellusb.v66.22486.

Machida, T., H. Matsueda, Y. Sawa, Y. Nakagawa, K. Hirotani, N. Kondo, K. Goto, T. Nakazawa, K. Ishikawa, and T. Ogawa (2008), Worldwide measurements of atmospheric CO_2 and other trace gas species using commercial airlines, *J. Atmos. Oceanic Technol.*, *25*, 1744–1754.

Maksyutov, S., et al. (2013), Regional CO_2 flux estimates for 2009–2010 based on GOSAT and ground-based CO_2 observations, *Atmos. Chem. Phys.*, *13*, 9351–9373.

O'Dell, C. W., et al. (2012), The ACOS CO_2 retrieval algorithm Part 1: Description and validation against synthetic observations, *Atmos. Meas. Tech.*, *5*, 99–121.

Oshchepkov, S., et al. (2012), Effects of atmospheric light scattering on spectroscopic observations of greenhouse gases from space: Validation of PPDF-based CO_2 retrievals from GOSAT, *J. Geophys. Res.*, *117*, D12305, doi:10.1029/2012JD017505.

Oshchepkov, S., et al. (2013), Effects of atmospheric light scattering on spectroscopic observations of greenhouse gases from space. Part 2: Algorithm intercomparison in the GOSAT data processing for CO_2 retrievals over TCCON sites, *J. Geophys. Res. Atmos.*, *118*, 1493–1512, doi:10.1002/jgrd.50146.

Peylin, P., et al. (2013), Global atmospheric carbon budget: Results from an ensemble of atmospheric CO_2 inversions, *Biogeosciences*, *10*, 6699–6720.

Reuter, M., et al. (2013), A joint effort to deliver satellite retrieved atmospheric CO_2 concentrations for surface flux inversions: The ensemble median algorithm EMMA, *Atmos. Chem. Phys.*, *13*, 1771–1780.

Reuter, M., et al. (2014), Satellite-inferred European carbon sink larger than expected, *Atmos. Chem. Phys. Discuss.*, *14*, 21,829–21,863, doi:10.5194/acpd-14-21829-2014.

Saeki, T., et al. (2013), Inverse modeling of CO_2 fluxes using GOSAT data and multi-year ground-based observations, *Sci. Online Lett. Atmos.*, *9*, 45–50, doi:10.2151/sola.2013-011.

Stephens, B. B., et al. (2007), Weak northern and strong tropical land carbon uptake from vertical profiles of atmospheric CO_2, *Science*, *316*, 1732–1735.

Stohl, A., C. Forster, A. Frank, P. Seibert, and G. Wotawa (2005), Technical note: The Lagrangian particle dispersion model FLEXPART version 6.2, *Atmos. Chem. Phys.*, *4*, 2461–2474.

Takagi, H., et al. (2014), Influence of differences in current GOSAT XCO_2 retrievals on surface flux estimation, *Geophys. Res. Lett.*, *41*, 2598–2605, doi:10.1002/2013GL059174.

Wofsy, S. C., et al. (2012), *HIPPO Merged 10-Second Meteorology and Atmospheric Chemistry and Aerosol Data (R_20121129)*, Carbon Dioxide Information Analysis Center, Oak Ridge National Laboratory and Oak Ridge and Tennessee. [Avaialble at http://dx.doi.org/10.3334/CDIAC/hippo_010, (Release 20121,129)].

Wunch, D., G. C. Toon, J. -F. L. Blavier, R. A. Washenfelder, J. Notholt, B. J. Connor, D. W. T. Griffith, V. Sherlock, and P. O. Wennberg (2011), The total carbon column observing network, *Philos. Trans. R. Soc.*, *369*, 2087–2112, doi:10.1098/rsta.2010.0240.

Yokota, T., Y. Yoshida, N. Eguchi, Y. Ota, T. Tanaka, H. Watanabe, and S. Maksyutov (2009), Global concentrations of CO_2 and CH_4 retrieved from GOSAT, first preliminary results, *Sci. Online Lett. Atmos.*, *5*, 160–163, doi:10.2151/sola.2009-041.

Yoshida, Y., et al. (2013), Improvement of the retrieval algorithm for GOSAT SWIR XCO_2 and XCH_4 and their validation using TCCON data, *Atmos. Meas. Tech.*, *6*, 1533–1547.